PHYSICAL REVIEW A VOLUME 6, NUMBER 4 OCTOBER 1972

Satellite Bands in Alkali-Atom Spectra*

G. D. Mahan
Department of Physics and Institute of Theoretical Science,
University of Oregon, Eugene, Oregon 97403

(Received 30 June 1971; revised manuscript received 24 April 1972)

A theoretical calculation is presented for absorption-line profiles of alkali-metal atomic spectra. The red- and violet-satellite bands caused by interactions with noble-gas perturbing atoms are discussed in detail. The statistical theory is used in calculating absorption profiles. It is shown that the pair-distribution function between atoms has an important, and temperature-dependent, influence on the red-satellite bands.

I. INTRODUCTION

In optical absorption experiments on alkali-metal atoms, the main transition takes an electron from the ground-state S orbital to an excited-state P orbital. Usually each transition has two primary absorption lines, associated with the $P_{1/2}$ and $P_{3/2}$ states, which are split into a doublet by the spin-orbit interaction. The absorption spectra may have additional structure, if other atoms are present in the gas. The case of noble-gas atoms perturbing the alkali-metal atoms has received much experimental and theoretical attention.[1-11] The experiments show that the two absorption lines of the alkali doublet are broadened and shifted. In addition, satellite absorption bands may appear on either side of the two main lines.

Extra absorption bands which appear on the high-frequency side of the $P_{3/2}$ line are blue satellites, while those on the low-frequency side of the $P_{1/2}$ line are red satellites. Hindmarsh and Farr[6] reviewed the properties of the red satellites, and proposed an explanation. Their calculations employed the statistical theory, which is a semiclassical theory which depends only upon the interatomic potentials between the alkali and noble gas. If $V_0(R)$ is the potential in the alkali ground S state, and $V_j(R)$ is the potential of the alkali excited P_j state, then $V_j'(R) = V_j(R) - V_0(R)$ is the difference potential. They assumed a Lennard–Jones form for $V_j'(R)$, and their calculations explained their experimental results on potassium perturbed by krypton.

The physics is quite simple. If an alkali atom undergoes an optical transition while a noble-gas atom is R away, then the photon energy required for the transition is $\hbar\omega = \hbar\omega_0 + V_j'(R)$, where $\hbar\omega_0$ is the transition frequency of the isolated alkali atom. A crude estimate of the absorption spectra is obtained by averaging over all possible coordinate positions R of the noble-gas atoms:

$$A(\omega) \simeq n \int d^3R \, g(R) \, \delta(\hbar\omega - \hbar\omega_0 - V_j'(R)) , \qquad (1.1)$$

where n is the density of noble-gas atoms. The factor $g(R)$ is the pair correlation function between the atoms.[12] The more elaborate version of the statistical theory (2.1) which is used in this article, considers interactions with more than one noble-gas atom at a time. The simplified version (1.1) is an accurate approximation when n is small, so that interactions with several noble-gas atoms at a time are rare events.

The present calculation extends the results of Hindmarsh and Farr in two ways. The first is that we have included a factor which they have omitted: the pair correlation function[12] between the positions of the atoms. The early versions[2,7,8] of statistical theory omitted this factor, but recent investigators[9-11] are starting to include it. In Sec. II we show that such a factor does belong. The results for a Lennard–Jones potential are presented in Sec. III. There it is shown that the pair correlation function may, under certain circumstances, suppress the intensity of the red-satellite band to the point where it may not be observed in the spectra. In other cases the pair correlation function may not affect the spectra at all.

The second part of our results are discussed in Sec. IV. There it is shown that a satellite band will result from any minimum or maximum in the difference potential $V_j'(R)$. It is shown that the results of Hindmarsh and Farr do not depend upon the choice of a Lennard–Jones potential. The same results are obtained from any difference potential $V_j'(R)$ which has a minimum with similar values of minimum energy ϵ_m, curvature K_m, and atomic separation R_m. The position of the satellite band occurs at an energy ϵ_m below the absorption line, while the relative intensity of the satellite band is determined by the factor $nR_m^2 K_m^{-1/2}$. For low values of n, these are the only two parameters which are determined, when experiment is compared to theory.

Satellite bands, can also occur from relative maxima in the difference potential $V_j'(R)$. This is of interest because recent calculations of the interatomic potential show relative maxima as well as minima.[5,10] In some cases these maxima can explain the position of the blue satellites.[5,10]

There have been numerous prior discussions on the relationship between $V_j'(R)$ and spectra.[2,7–9,11] The important result of the present calculations is that satellite bands provide direct information on the existence of maxima or minima in $V_j'(R)$. The energy position of satellite bands, relative to the main absorption lines, is a direct measure of extremal energy ϵ_m. This agrees with experimental observations that satellite-band positions are independent of temperature T and n.[6]

II. STATISTICAL THEORY

An important idea in our statistical theory is that the alkali and perturbing atom can not get too close to each other. This arises because of the mutual repulsion they feel at close distances. The physical function describing this behavior is the pair distribution function $g_{12}(R)$,[12] which is the probability that a noble-gas atom is at R, if the alkali is at $R=0$.

Since we have a binary fluid, there are other distribution functions $g_{11}(R)$ between noble-gas pairs and $g_{22}(R)$ between alkali pairs.

Our result for the absorption spectra in the statistical theory has the form

$$\begin{aligned} A(\omega) &= \sum_j \int_{-\infty}^{\infty} \frac{dt}{2\pi} \exp[i(\omega-\omega_j)t - \phi_j(t)] , \\ \phi_j(t) &= n \int d^3R\, g_{12}(R)\left(1 - e^{-itV_j'(R)}\right) , \end{aligned} \tag{2.1}$$

where n is the noble-gas density.

The early versions of the statistical theory omitted the $g_{12}(r)$ factor. Recent articles have started to include this factor. Only Futrelle[11] has suggested a reason why this factor needs to be included, and his derivation is quite complicated. This section presents a simple derivation of (2.1) It is assumed the atoms in the gas behave as a classical fluid. The derivation employs the functional derivative techniques developed by Percus for classical fluids.[12]

If the density of alkali atoms is much less than the density of noble gas atoms, then each alkali is surrounded by only noble-gas atoms. In the statistical theory, for each absorption band j, one wants to evaluate an integral of the form

$$A_j(\omega) = \int_{-\infty}^{\infty} \frac{dt}{2\pi} e^{it(\omega-\omega_j)} \int \prod_l d^3R_l\, e^{-iV_j'(t)} \times P(\vec{R}_1, \vec{R}_2, \vec{R}_3, \ldots, \vec{R}_N) , \tag{2.2}$$

where $P(\vec{R}_1, \vec{R}_2, \ldots, \vec{R}_N)$ is the probability that one perturbing atom is at $\vec{R}_1$, a second at $\vec{R}_2$, etc. For a classical fluid, this function is

$$P(\vec{R}_1, \vec{R}_2, \ldots, \vec{R}_N) = \exp\Big[-\beta \sum_l V_0(\vec{R}_l) - \tfrac{1}{2}\beta \sum_{l,m} U(\vec{R}_l - \vec{R}_m)\Big] / \Xi(\beta V_0) ,$$

$$\Xi(\beta V_0) = \int \prod_l d^3R_l\, P(\vec{R}_1, \vec{R}_2, \ldots, \vec{R}_N) ,$$

where $U(\vec{R})$ is the interaction between the noble-gas atoms, and $V_0(\vec{R})$ is the interaction between the alkali atom is its ground state and the noble-gas atom. We can rewrite (2.2) as

$$A_j(\omega) = \int_{-\infty}^{\infty} \frac{dt}{2\pi} e^{+it(\omega-\omega_j)} \frac{\Xi(\beta V_0 + itV_j')}{\Xi(\beta V_0)} .$$

By using the theory of functional derivatives, Percus[12] has shown that this may be evaluated from the series

$$\begin{aligned} &\ln\Xi(\beta V_0 + itV_j') - \ln\Xi(\beta V_0) \\ &\quad = \int d^3R_1\, \mathfrak{F}(\vec{R}_1)\left(e^{-itV_j'(\vec{R}_1)} - 1\right) \\ &\qquad + \tfrac{1}{2} \int d^3R_1\, d^3R_2\, \mathfrak{F}(\vec{R}_1, \vec{R}_2)\left(e^{-itV_j'(R_1)} - 1\right) \\ &\qquad \times \left(e^{-itV_j'(R_2)} - 1\right) + \cdots . \end{aligned} \tag{2.3}$$

We keep only the first term on the right-hand side, as is conventional, and then identify[12] $\mathfrak{F}(\vec{R}_1) = n g_{12}(\vec{R}_1)$. Thus we have derived (2.1). For the present numerical calculations, we have used the simple approximation[12]

$$g_{12}(\vec{R}) = e^{-\beta V_0(R)} . \tag{2.4}$$

In this form of the statistical theory, the absorption spectra (2.1) no longer depends upon just the difference of the ground- and excited-state potential curves, but also upon the ground-state potential alone. One advantage of the present derivation is that (2.3) provides a formula for improving the approximation at increased densities by retaining additional terms. At increased densities n, one can also improve upon (2.4) by obtaining $g_{12}(R)$ from the Percus–Yevick equation.[12]

III. LENNARD-JONES POTENTIAL

The integrals in (2.1) may be evaluated for the case of a Lennard–Jones potential in the initial and final state. So we take

$$V_0(R) = 4\sigma_0\left[\left(\frac{a_0}{R}\right)^{12} - \left(\frac{a_0}{R}\right)^{6}\right] = \frac{C_{12}^{(0)}}{R^{12}} - \frac{C_6^{(0)}}{R^6} , \tag{3.1a}$$

$$V_j(R) = 4\sigma_j\left[\left(\frac{a_j}{R}\right)^{12} - \left(\frac{a_j}{R}\right)^{6}\right] = \frac{C_{12}^{(j)}}{R^{12}} - \frac{C_6^{(j)}}{R^6} , \tag{3.1b}$$

and

$$V_j' = V_j - V_0 = 4\sigma'\left[\left(\frac{a'}{R}\right)^{12} - \left(\frac{a'}{R}\right)^{6}\right]$$

$$= \frac{C'_{12}}{R^{12}} - \frac{C'_6}{R^6}\,. \qquad (3.2)$$

We are assuming that the initial, final, and difference potential are all of the Lennard–Jones type. The assumption is not always in accord with the actual physical situation. As an example of a situation where this does not apply, consider the case that V_0 has a stronger repulsive term than V_j. Then the coefficient C'_{12} is negative. Since in optical absorption one usually has $C'_6 > 0$, this example has V'_j purely negative, with no minimum! However, we shall not consider this case, but shall restrict ourselves to (3.1) and (3.2).

We wish to evaluate (2.1) as the following:

$$A(\omega) = \int_{-\infty}^{\infty} \frac{dt}{2\pi}\ \exp[i(\omega-\omega_0)t - \phi(t)],$$
$$\phi(t) = n \int d^3R\, e^{-\beta V_0(R)}(1 - e^{-itV'_j(R)})\,. \qquad (3.3)$$

Since $\phi^*(t) = \phi(-t)$, it is sufficient to evaluate just the real part of $A(\omega)$:

$$A(\omega) = \mathrm{Re}\int_0^{\infty} (dt/\pi)\exp[i(\omega-\omega_0)t - \phi(t)]\,. \qquad (3.4)$$

The integral (3.3), with Lennard–Jones potentials (3.1) and (3.2), is similar to that evaluated by Hindmarsh and Farr.[6] Following their method yields

$$\phi(t) = C(T) - \lambda\gamma^{1/4}[\Gamma(-\tfrac14)F(-\tfrac14,\tfrac12,z) + 2z^{1/2}\Gamma(\tfrac14)F(\tfrac14,\tfrac32,z)]\,, \qquad (3.5)$$

$$C(T) = \lambda\, 2^{1/2} b^{1/4}[\Gamma(-\tfrac14)F(-\tfrac14,\tfrac12,b) + 2b^{1/2}\Gamma(\tfrac14)F(\tfrac14,\tfrac32,b)]\,. \qquad (3.6a)$$

$$C(T) = \lambda\pi b^{1/4}\, 2^{7/4}\, e^{b/2}\, V(-1,(2b)^{1/2})\,, \qquad (3.6b)$$

$$b = \beta\sigma_0, \qquad \lambda = \tfrac13 \pi n a_0^3, \qquad \lambda' = \tfrac13\pi n(a')^3\,, \qquad (3.7)$$

$$\gamma = 4\beta\sigma_0 + i4t\sigma'(a'/a_0)^{12} = [\beta C_{12}^{(0)} + itC'_{12}]\,a_0^{-12}\,,$$
$$z = \frac{[\beta\sigma_0 + it\sigma'(a'/a_0)^6]^2}{\beta\sigma_0 + it\sigma'(a'/a_0)^{12}} = \frac{[\beta C_6^{(0)} + itC'_6]^2}{4[\beta C_{12}^{(0)} + itC'_{12}]}\,, \qquad (3.8)$$

where $\Gamma(\pm\frac14)$ are γ functions, and $F(-\frac14,\frac12,z)$ are confluent hypergeometric functions.[12] The result of Hindmarsh and Farr is obtained by setting $\beta = 0$. This would eliminate the factor $g_{12} = e^{-\beta V_0}$, which they omitted.

This is a complicated result for $\phi(t)$. It would be cumbersome to evaluate explicitly. However, one of our main points is that a very simple approximation pertains in many situations. This occurs if the perturbation density n is moderately low, say around one atmosphere. Then the dimensionless constant λ is only of order 10^{-3}. This is quite small. It means that $\phi(t)$ is negligibly small unless z is large, which means that t is large. So at these moderate densities of perturbers, we only need to consider the asymptotic limit of $\phi(t)$ as $t\to\infty$. We get

$$\lim_{t\to\infty} z = it\sigma' + \delta + O\left(\frac{1}{t}\right)\,, \qquad (3.9)$$

where

$$\delta = \beta\sigma_0\left[2\left(\frac{a_0}{a'}\right)^6 - \left(\frac{a_0}{a'}\right)^{12}\right] = -\beta V_0(R_m)\,. \qquad (3.10)$$

The parameter δ is an important aspect of our result. The difference potential $V'_j(R)$ has its minimum at $R_m = 2^{1/6}a'$. So δ is proportional to the value of the ground-state potential evaluated at the minimum of the difference potential. It may be either positive or negative.

Using (3.9) in (3.5) gives

$$\lim_{t\to\infty}\phi(t) = C(T) + \lambda'\left\{8(\pi\sigma' t)^{1/2}e^{-i\pi/4} - 2\left(\frac{2\pi}{\sigma' t}\right)^{1/2}\exp[i(\sigma' t - \tfrac14\pi) + \delta] + \left(\frac{4\pi}{\sigma' t}\right)^{1/2} e^{-i\pi/4}\left[1 + 2\beta\sigma_0\left(\frac{a_0}{a'}\right)^6\right] + O(t^{-3/2})\right\}. \qquad (3.11)$$

Let us examine these various terms. The constant term $C(T)$ is going to be small if λ is small, unless $\beta\sigma_0$ has anomalously large values. This is plotted in Fig. 1 as a function of $b = \beta\sigma_0$.

In (3.6a) and (3.6b) we have listed two equivalent formulas for $C(T)$. The first is useful because it shows that $\phi(t) = 0$ at $t = 0$. The second is more useful for numerical computation. The parabolic cylinder function $V(-1, x)$ is tabulated.[13] The function $C(T)$ grows exponentially with b. This is obvious from its asymptotic expansion

$$\lim C(T) = 2\lambda(2\pi/b)^{1/2}e^b \quad \text{as } T\to 0\,.$$

The insert in Fig. 1 shows that $C(T)$ is negative for small values of b.

The second term in $\phi(t)$ may be rewritten as

$$\phi_2(t) = \tfrac43\pi^{3/2}n(C'_6 t)^{1/2}e^{-i\pi/4}. \qquad (3.12)$$

This term, which was first derived by Kuhn,[7] is just the contribution from the van der Waals forces. That is, we could derive $\phi_2(t)$ by just taking $V'_j(R) = -C'_6/R^6$, $g_{12} = 1$,

$$\phi_2(t) = n\int d^3R\,[1 - e^{itC'_6/R^6}]\,.$$

If this term alone is used in evaluating $A(\omega)$, there results Kuhn's $(\omega_0-\omega)^{-3/2}$ red tail to the spectral line

$$A_2(\omega) = \mathrm{Re}\int_0^{\infty}\frac{dt}{\pi}\ \exp[i(\omega-\omega_0)t - \phi_2(t)]\,,$$

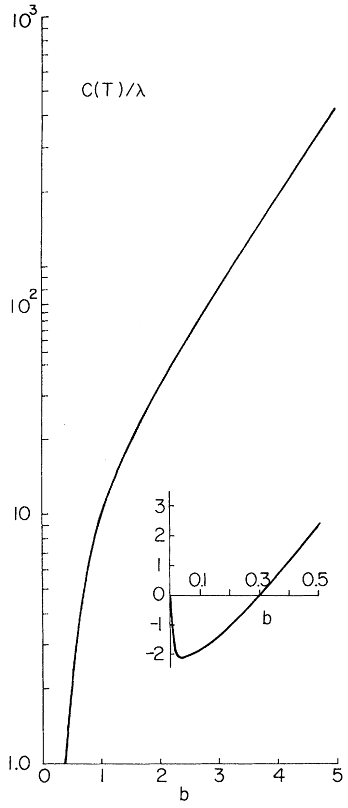

FIG. 1. Plot of $C(T)/\lambda$ as a function of $b=\sigma_0/k_BT$, where σ_0 is the depth of the Lennard–Jones potential for the ground state. The functional form for $C(T)$ is given in (3.6b).

$$A_2(\omega)=\frac{1}{\Omega}\left[\frac{\Omega_0}{\pi\Omega}\right]^{1/2} e^{-\Omega_0/\Omega}\,\Theta(\Omega)\,, \tag{3.13}$$

$$\Omega=\omega_0-\omega,\ \ \Omega_0=\tfrac{4}{9}\pi^3 n^2 C_6'\,, \tag{3.14}$$

where $\Theta(\Omega)$ is the step function. These results are well known.

The third term in (3.11) has very little dependence upon the Lennard–Jones potential. This term occurs whenever there is a difference potential minimum of any kind. We only need to assume that a difference potential minimum exists. So if we take $V_j'(R)$ to have a minimum at R_m,

$$V_j'(R)=-\sigma'+\tfrac{1}{2}K(R-R_m)^2\,, \tag{3.15}$$

where K is the positive curvature, then the integral

$$\phi_3(t)=n\int d^3R\,(1-\exp\{-it[-\sigma'+\tfrac{1}{2}K(R-R_m)^2]\}) \tag{3.16}$$

yields

$$\phi_3(t)=-4\pi nR_m^2(2\pi/Kt)^{1/2}\exp(+it\sigma'-\tfrac{1}{4}i\pi)\,. \tag{3.17}$$

Since the curvature of the Lennard–Jones potential is

$$K=72\sigma'/R_m^2\,,$$

then (3.17) is the same expression as the third term in (3.11). The only difference between the two is the important factor e^6. We could have gotten this factor in (3.17), if we had put the factor $g_{12}(Rm)=e^{-\beta V_0(R_m)}$ into (3.16). That is, we evaluate the pair-distribution function $g_{12}(R)$ at the minimum R_m of the difference potential. This would then give in (3.17) exactly the third term in (3.11)

$$\phi_3(t)=-4\pi nR_m^2(2\pi/Kt)^{1/2}\exp[i(t\sigma'-\tfrac{1}{4}\pi)-\beta V_0(R_m)]\,. \tag{3.18}$$

This is the term which gives the red-satellite bands. If we consider the integral for this term alone, we have

$$A_3(\omega)=\mathrm{Re}\int_0^\infty\frac{dt}{\pi}\,e^{it(\omega-\omega_0)}\,e^{-\phi_3(t)}\,.$$

The integral is hard to do. So we expand

$$A_3(\omega)=\mathrm{Re}\int_0^\infty\frac{dt}{\pi}\,e^{it(\omega-\omega_0)}[1-\phi_3(t)+\cdots]\,.$$

The term proportional to $\phi_3(t)$ gives an estimate of the red-satellite band

$$A_3(\omega)=4\pi nR_m^2(2/K\Omega)^{1/2}\,\Theta(\Omega)\,e^{-\beta V_0(R_m)}\,,$$

$$\Omega=\omega-\omega_0+\sigma'\,.$$

This is nearly the same result which is obtained in the simpler version of the statistical theory (1.1)

$$A_3(\omega)\simeq n\int d^3R\,e^{-\beta V_0(R)}\,\delta(\hbar\omega-\hbar\omega_0-V_j'(R))\,, \tag{3.19}$$

where $V_j'(R)$ is the form in (3.15).

The last term in (3.11) will not be discussed in detail. It appears to be a renormalization term which reduces the intensity of the main absorption line as the satellite band is increased.

Most of these results, which we have just discussed, are already known. The new result we wish to emphasize is that one should combine the effects of these various contributions to $\phi(t)$. So a much better approximation to $A(\omega)$ should be given by simultaneously including both $\phi_2(t)$ and $\phi_3(t)$:

$$A(\omega)=e^{-C(T)}\,\mathrm{Re}\int_0^\infty\frac{dt}{\pi}$$
$$\times\exp[i(\omega-\omega_0)t-\phi_2(t)][1-\phi_3(t)]\,,$$

$$A(\omega)=e^{-C(T)}A_2(\omega)+4nR_m^2(2\pi/K)^{1/2}$$
$$\times\exp[-C(T)-\beta V_0(R_m)]I_1(\omega-\omega_0+\sigma')\,,$$

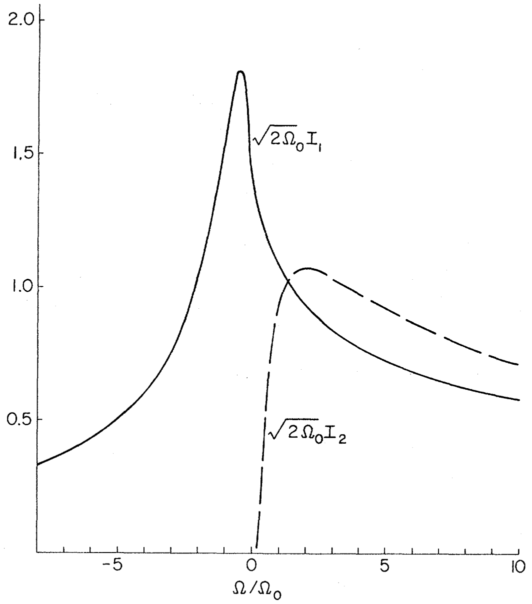

FIG. 2. Plot of the satellite-band profiles I_1 and I_2. Both are plotted for a potential minimum. They differ only in the sign of the van der Waals coefficient.

$$I_1(\Omega)=\mathrm{Re}\, e^{i\pi/4}\int_0^\infty \frac{dt}{t^{1/2}}\, e^{it\Omega} \exp[-(1-i)(2t\Omega_0)^{1/2}], \tag{3.20}$$

where $A_2(\omega)$ and Ω_0 are given in (3.13) and (3.14). The integral for $I_1(\Omega)$ may be done, and the results are expressed in terms of Dawson's Integral F and the complementary error function[13] Thus we have

$$I_1(\Omega)=\frac{2}{(|\Omega|)^{1/2}}\, F\left(\left(\frac{\Omega_0}{|\Omega|}\right)^{1/2}\right)\theta(-\Omega)+\left(\frac{\pi}{\Omega}\right)^{1/2} e^{\Omega_0/\Omega} \times \mathrm{erfc}\left(\left(\frac{\Omega}{\Omega_0}\right)^{1/2}\right)\theta(\Omega). \tag{3.21}$$

A plot of the function $I_1(\Omega)$ is shown in Fig. 2. There is a peak in the line profile. This peak is the red-satellite band centered near $\omega=\omega_0-\sigma'$. It is the same band which was discussed by Hindmarsh and Farr.[6] Their results were obtained by numerical integration of (3.4) and (3.5), whereas we have obtained an analytical result (3.21), which is valid for low density of perturber atoms.

Our calculations also show that the red-satellite band has temperature-dependent factors. The term $C(T)$ is probably not important at low n, however, the factor $g_{12}=e^{-\beta V_0(R_m)}$ could be very important. For example, if the minimum R_m was in the region where $V_0(R)$ is strongly repulsive, then this factor g_{12} would be very small. This would suppress the satellite band entirely. This could explain why the red-satellite band is often missing from some alkali spectra for some noble-gas perturbers. Another possibility is that $V_0(R_m)$ has a moderate value, so that $\beta V_0(R_m)$ is of order unity. Then the strength of the satellite band will have a temperature dependence. The satellite band intensity could either increase or decrease with temperature, depending upon the sign of $V_0(R_m)$.

IV. OTHER POTENTIALS

In order to calculate line profiles, we need to know the time dependence of $\phi(t)$. However, at low density of perturber, it is sufficient to know how $\phi(t)$ behaves at large values of t. We just showed, for the Lennard-Jones potential, that $\phi(t)$ had two main contributions at large t. One was from the attractive van der Waals tail, and the other from the potential minimum. Other aspects of the potential, such as the hard-core repulsive region, are unimportant as their t dependence falls off faster than $t^{-1/2}$.

We suggest that this must be a feature of line profiles from all interatomic potentials. The two important features are the van der Walls region, and the contribution from potential minima and maxima. We shall show that potential maxima cause the same effects as potential minima. Other aspects of the potential, such as the hard-core repulsive region, do not influence the result. This is regrettable, as this means that experimental line shapes are not able to provide much information about these other parts of the potential. One should keep in mind that these conclusions only apply in the low-density region.

Futrelle[11] has discussed a unified line-shape theory, wherein he tries to hybridize the impact and statistical theory. One interesting result he suggests is that at large t, the exact function $\phi_{\text{exact}}(t)$ is the sum of statistical theory $\phi(t)$ and impact theory $-i(\Sigma_R+i\Sigma_I)t$, where Σ_R is the line shift and Σ_I is the linewidth:

$$\lim_{t\to\infty}\phi_{\text{exact}}(t)=\lim_{t\to\infty}[\phi(t)-i(\Sigma_R+i\Sigma_I)t] .$$

This implies that our asymptotic form for $\phi(t)$ could be improved at large by adding the impact contributions $-(\Sigma_R+i\Sigma_I)t$. Although we accept this as a reasonable result, we shall not follow it in these calculations as it introduces two additional parameters Σ_R and Σ_I into the computations. It should probably be done for actual comparisons to experimental data. This procedure was used by Hindmarsh and Farr in their computations. They Lorenzian-broadened their statistical results, which is equivalent to adding the $\Sigma_I t$ term to $\phi(t)$. It is easy to include these terms in our result. In (3.21) the frequency Ω is replaced by the complex frequency $\Omega-\Sigma_R-i\Sigma_I$, and one takes the real part of the result.

We showed that the van der Waals potential is a major contribution to $\phi(t)$ in the statistical theory. This contribution $\phi_2(t)$ is given in (3.12) for the case that $C_6' = C_6^{(j)} - C_6^{(0)} > 0$. The other possibility is that $C_6' < 0$. Then one gets that

$$\tfrac{4}{3}\pi^{3/2} n\,(-\,|C_6'|\,t)^{1/2} e^{-i\pi/4} = \tfrac{4}{3}\pi^{3/2} n(|C_6'|\,t)^{1/2} e^{i\pi/4}\,.$$

If we denote the sign of a quantity x as $\mathrm{sgn}(x)$, then the general form for $\phi_2(t)$ is

$$\phi_2(t) = \tfrac{4}{3}\pi^{3/2} n[t\,|C_6'|\,]^{1/2} \exp[-\tfrac{1}{4} i\pi\,\mathrm{sgn}(C_6')]\,.$$

The other major contribution to $\phi(t)$ comes from the minima and maxima in the difference potential $V_j'(R)$. Each extrema is characterized by three constants: the position R_m, the extremal energy ϵ_m, and the curvature K_m. Thus we have

$$V_j'(R) = \epsilon_m + \tfrac{1}{2} K_m (R - R_m)^2 \quad \text{if} \quad R \sim R_m\,.$$

The energy ϵ_m may have either sign, and we shall adopt the convention that $\epsilon_m > 0$ for extrema at positive energies. The curvature K_m is positive for a minimum and negative for a maximum. The contribution to $\phi(t)$ is

$$\phi_m(t) = -4\pi n R_m^2 \left(\frac{2\pi}{t\,|K_m|}\right)^{1/2} \exp[-it\epsilon_m - \beta V_0(R_m) - \tfrac{1}{4} i\pi\,\mathrm{sgn}(K_m)]\,. \tag{4.1}$$

The sign of the factor $e^{-i\pi/4}$ depends upon the sign of K_m. The total value of $\phi(t)$ is obtained by summing over all extrema

$$\lim_{t\to\infty} \phi(t) = C(T) + \phi_2(t) + \sum_m \phi_m(t)\,.$$

The line-shape profile $A(\omega)$ is obtained, as before, by linearizing the contributions from $\phi_m(t)$:

$$A(\omega) = \mathrm{Re}\int_0^\infty \frac{dt}{\pi} \exp[i(\omega - \omega_0)t - C(T) - \phi_2(t)] \times [1 - \sum_m \phi_m(t)]\,, \tag{4.2}$$

$$A(\omega) = A_2(\omega)\, e^{-C(T)} + \textstyle\sum_m A_m(\omega)\,. \tag{4.3}$$

The result for $A_2(\omega)$ has been given in (3.13) for the case of $C_6' > 0$. The result for $C_6' < 0$ is similar, the only difference is that $\Omega = \omega - \omega_0$, since the band tail is now on the violet side of the resonance frequency. This situation $C_6' < 0$ is not encountered very often in experimental absorption spectra.

In (4.3), each $A_m(\omega)$ describes a satellite band in the absorption spectra. A red band occurs if $\epsilon_m < 0$, and a violet band occurs if $\epsilon_m > 0$. A satellite band occurs for both potential minima and maxima, and a minima or maxima can each occur for either sign of ϵ_m.

TABLE I. Satellite-band profiles.

	$K_m > 0$	$K_m < 0$
$c_6' > 0$	$I_1(\omega - \omega_0 - \epsilon_m)$	$I_2(\omega - \omega_0 - \epsilon_m)$
$c_6' < 0$	$I_2(\omega_0 + \epsilon_m - \omega)$	$I_1(\omega_0 + \epsilon_m - \omega)$

In general, additional satellite bands can occur at higher harmonics of these basic frequencies, at multiples of ϵ_m, and also at the various combinations $\epsilon_n \pm \epsilon_m$, etc. Our theory does not describe these harmonics, because we have linearized our formula

$$\exp(-\textstyle\sum_m \phi_m) = 1 - \sum_m \phi_m\,.$$

However, the intensity of these harmonics will be small as long as $4\pi n R_m^3$ is small. They may be neglected since we are confining our discussion to the case where n is small at low perturber pressures.

There are two parameters in the theory whose sign are important, C_6' and K_m. The two choices of sign for each quantity lead to four classes of behavior. One of these, $C_6' > 0$ and $K_m > 0$, was discussed in the previous section. It gives a line shape of the form

$$A_m(\omega) = 4n R_m^2 (2\pi/K_m)^{1/2} e^{-C(T)} e^{-\beta V_0(R_m)} \times I_1(\omega - \omega_0 - \epsilon_m)\,, \tag{3.20}$$

where $I_1(\Omega)$ is given in (3.21). The other important case which will be encountered in absorption spectra is $C_6' > 0$, $K_m < 0$, a potential maximum. Here we get

$$A_m(\omega) = 4n R_m^2 (2\pi/|K_m|)^{1/2} e^{-C(T)} e^{-\beta V_0(R_m)} \times I_2(\omega - \omega_0 - \epsilon_m)\,,$$

$$I_2(\Omega) = \mathrm{Re}\, e^{i\pi/4} \int_0^\infty \frac{dt}{t^{1/2}} e^{it\Omega} \exp[-(1 - i)(2t\Omega_0)^{1/2}]\,. \tag{4.4}$$

The integral for I_2 may be done and gives

$$I_2(\Omega) = (\pi/|\Omega|)^{1/2} e^{-\Omega_0/|\Omega|}\, \theta(-\Omega)\,. \tag{4.5}$$

This is basically a square-root singularity, except for the exponential factor which is negligible except very near the satellite band frequency. The frequency dependence of $I_1(\Omega)$ and $I_2(\Omega)$ are quite different. This difference primarily arises from the influence of the van der Waals contribution. The $I_2(\Omega)$ form is essentially similar to that calculated (3.19) in the absence of the van der Waals term. One choice for the sign of C_6' leads to qualitatively different line shapes $I_1(\Omega)$ for the satellite band than does the other $I_2(\Omega)$.

The four classes of behavior, depending upon the signs of C_6' and K_m, each have either the $I_1(\Omega)$ or $I_2(\Omega)$ frequency dependence. These choices are summarized in Table I. Figure 2 shows plots of I_1 and I_2. They are calculated with the same set of parameters and only differ in the sign of C_6'. What is actually plotted in Fig. 2 are the dimensionless functions $(2\Omega_0)^{1/2} I_1$ and $(2\Omega_0)^{1/2} I_2$. The parameters are chosen to represent a potential minimum $K_m > 0$, while I_1 has $C_6' > 0$ and I_2 has $C_6' < 0$. The shapes of the two curves are quite different. The case I_1 has a much sharper satellite band profile. In Fig. 2, the frequency is measured in units of Ω_0. For low-perturber densities, say about 1 atm, then Ω_0 is very small—it is a small fraction of an cm^{-1} unit. In this case one can perhaps ignore the small differences between I_1 and I_2 and use

$$\lim_{n \to 0} I_1 \simeq I_2 \simeq \left(\frac{\pi}{|\Omega|} \right)^{1/2} \Theta(\Omega \operatorname{sgn}(K_m)) \cdot$$

Of course, this is the same result as obtained in (3.19), where the van der Waals contribution was omitted. Effects dependent upon Ω_0/Ω may be observable at high concentrations.

We conclude this section by again emphasizing the importance of the factor $e^{-\beta V_0(R_m)}$. This factor could cause a red-satellite band to have great temperature sensitivity. It could also explain why some alkali-noble gas pairs do not show red-satellite bands at low density, $g_{12}(R_m) \sim 0$ if $R_m < a_0$.

---

*Research supported by a grant from the National Science Foundation.

[1] O. Oldenberg, Z. Physik 47, 184 (1928); 55, 1 (1929); H. Kuhn and O. Oldenberg, Phys. Rev. 41, 72 (1932).

[2] L. Klein and H. Margenau, J. Chem. Phys. 30, 1556 (1959); H. Margenau, Phys. Rev. 82, 156 (1951).

[3] S. Y. Ch'en and M. Takeo, Rev. Mod. Phys. 29, 20 (1957); S. Y. Ch'en, in Proceedings of the International Conference on Optical Pumping and Line Shape, Warsaw, 1968 (unpublished); D. E. Gilbert and S. Y. Ch'en, Phys. Rev. 188, 40 (1969).

[4] S. Y. Ch'en and R. A. Wilson, Jr., Physica 27, 497 (1961).

[5] W. E. Baylis, J. Chem. Phys. 51, 2665 (1969); JILA Report No. 100 (unpublished); private communication.

[6] W. R. Hindmarsh and J. M. Farr, J. Phys. B 2, 1388 (1969); D. G. McCarten and W. R. Hindmarsh, *ibid.* 2, 1396 (1969).

[7] H. G. Kuhn, *Atomic Spectra* (Academic, New York, 1962).

[8] O. Jefimenko, J. Chem. Phys. 37, 2125 (1962); 42, 205 (1965); O. Jefimenko and G. M. Williams, *ibid.* 42, 207 (1965).

[9] H. C. Jacobson, Phys. Rev. A 4, 1363, 1368 (1971).

[10] G. D. Mahan, Phys. Letters 39A, 145 (1972).

[11] R. P. Futrelle, Phys. Rev. A 5, 2162 (1972).

[12] J. K. Percus, in *Classical Fluids*, edited by H. L. Frisch and J. L. Lebowitz (Benjamin, New York, 1964). My Equation (23) may be deduced from Eqs. (4.17), (4.20), and (4.22) of this reference.

[13] *Handbook of Mathematical Functions*, edited by M. Abramowitz and J. A. Stegun (U.S. GPO, Washington, D.C., 1964).